

# EXPLOITING BLOCK TRIANGULAR SUBMATRICES IN KKT SYSTEMS \*

ROBERT PARKER<sup>†</sup>, MANUEL GARCIA<sup>†</sup>, AND RUSSELL BENT<sup>†</sup>

**Abstract.** We propose a method for solving Karush-Kuhn-Tucker (KKT) systems that exploits block triangular submatrices by first using a Schur complement decomposition to isolate the block triangular submatrices then performing a block backsolve where only diagonal blocks of the block triangular form need to be factorized. We show that factorizing reducible symmetric-indefinite matrices with standard  $1 \times 1$  or  $2 \times 2$  pivots yields fill-in outside the diagonal blocks of the block triangular form, in contrast to our proposed method. While exploiting a block triangular submatrix has limited fill-in, unsymmetric matrix factorization methods do not reveal inertia, which is required by interior point methods for nonconvex optimization. We show that our target matrix has inertia that is known *a priori*, letting us compute inertia of the KKT matrix by Sylvester’s law. Finally, we demonstrate the computational advantage of this method on KKT systems from optimization problems with neural network surrogates in their constraints. Our method achieves up to  $15 \times$  speedups over state-of-the-art symmetric indefinite matrix factorization methods MA57 and MA86 in a constant-hardware comparison.

**Key words.** Symmetric-indefinite matrices, interior point methods, neural networks, block triangular matrices, Schur complement

**MSC codes.** 15B99, 65F05, 65F50

**1. Introduction.** Factorizing symmetric, indefinite Karush-Kuhn-Tucker (KKT) matrices is a computational bottleneck in interior point methods for nonconvex, local optimization. Methods for solving the KKT linear system can be grouped into three broad categories:

1. Direct methods,
2. Iterative methods, and
3. Decomposition methods (including Schur complement and null space decompositions).

Interior point methods for nonconvex optimization most commonly use direct methods for solving their KKT systems. These methods factorize the matrix into the product  $LBL^T$ , where  $L$  is lower triangular and  $B$  is block-diagonal with a combination of  $1 \times 1$  and  $2 \times 2$  blocks. These blocks correspond to  $1 \times 1$  or  $2 \times 2$  pivots selected by the method of Bunch and Kaufman [8]. The factors are typically computed by multifrontal [24] or supernodal [45] methods, which have been implemented in several widely-used codes, e.g., MA57 [22], MA86 [36], MA97 [37], UMFPACK [19], and others.

Iterative methods (e.g., Krylov subspace methods) have also been used to solve KKT systems [4, 17]. These methods do not require storing the matrix or its factors in memory simultaneously and their repeated matrix-vector multiplications can be parallelized on GPUs. However, the ill-conditioning encountered in interior point methods leads to slow convergence [67], making these methods less popular in interior point implementations, especially for nonconvex optimization. Nonetheless, iterative linear solvers for interior point methods are an active area of research, with work focused on improving preconditioning [10, 57] and analyzing the impact of inexact linear algebra [66].

---

\*Submitted to the editors DATE.

**Funding:** Funded by the Los Alamos National Laboratory LDRD program. LA-UR-26-20941.

<sup>†</sup>Los Alamos National Laboratory, Los Alamos, NM

Decomposition methods exploit the block structure of the KKT matrix,

$$\text{KKT} = \begin{bmatrix} A & B^T \\ B & \end{bmatrix},$$

to decompose the linear system solve into solves involving smaller systems. These smaller systems may then be solved with either direct or iterative methods. Null space methods are decompositions that exploit a partition of variables into “dependent variables” and “degrees of freedom” in order to compute a basis for the null space of  $B$  [4, 15]. This basis is then used to reduce the KKT system to a smaller system in the dimension of the number of degrees of freedom (the number of variables minus the number of equality constraints). These methods are typically effective if the number of degrees of freedom is small, although constructing the null space basis can also be a bottleneck. To overcome this bottleneck in the context of transient stability constrained optimal power flow, Geng et al. [28, 29] have exploited a block triangular decomposition for the unsymmetric solve required to construct the null space basis.

Schur complement methods exploit the nonsingularity of one or more symmetric submatrices of the KKT matrix to decompose the linear system solve into multiple smaller solves. Benzi et al. [4] describe a basic Schur complement method exploiting the nonsingularity of  $A$ . A similar method relying on regularization of  $A$  has been described by Golub and Grief [30] and implemented in the HyKKT solver [56] using a direct method to construct the Schur complement and an iterative method to solve the system involving the Schur complement matrix. In contrast to these general-purpose Schur complement methods, many such methods have exploited problem-specific structures to factorize KKT matrices in parallel. For linear programs, Gondzio and Sarkissian [31], Grigoriadis and Khachiyan [33], Lustig and Li [48], and others have exploited decomposable block structures in interior point methods. In the context of nonconvex optimization, Wright [65] and Jin et al. [40] have exploited nonsingular diagonal blocks in block tridiagonal matrices, while Laird and Biegler [43] have exploited independent submatrices due to distinct scenarios in stochastic optimization and Kang et al. [41] have exploited nonsingular submatrices at each time point in dynamic optimization.

Our contribution is a Schur complement method that, instead of exploiting many independent, nonsingular submatrices, exploits a single nonsingular submatrix that has a favorable structure for factorization and backsolves. The structure we exploit is a block triangular structure (see Subsection 2.4) that allows us to limit fill-in to diagonal blocks of this block triangular form, which is not possible when factorizing these same systems with standard direct methods. Specifically, we:

1. Propose a novel combination of symmetric Schur complement and unsymmetric block triangular decomposition algorithms,
2. Demonstrate that standard  $1 \times 1$  and  $2 \times 2$  pivoting leads to fill-in outside the diagonal blocks of block triangular submatrices,
3. Prove that regularization on the relevant block in our KKT matrices is both undesirable and unnecessary, and
4. Demonstrate the computational advantage of our approach on KKT matrices derived from optimization problems with neural network constraints. (See [11, 58, 46] for background and applications of these optimization problems.)

Our results show that exploiting one large submatrix with a special structure can be advantageous in Schur complement methods for symmetric, indefinite systems. While parallel computing is outside the scope of this work, we note that exploiting a single large, nonsingular submatrix has potential to exploit GPU acceleration as data

transfer overhead is low compared to the potential speedup that can be gained by processing this submatrix in parallel.

## 2. Background.

**2.1. Interior point methods.** We consider symmetric indefinite linear systems from interior point methods for solving nonlinear optimization problems in the form given by Equation (2.1):

$$(2.1) \quad \begin{aligned} \min_x \quad & \varphi(x) \\ \text{subject to} \quad & f(x) = 0 \\ & x \geq 0 \end{aligned}$$

Here,  $x$  is a vector of decision variables and functions  $\varphi$  and  $f$  are twice continuously differentiable. We note that this formulation does not preclude general inequalities; for our purposes, we assume they have already been reformulated with a slack variable. Interior point methods converge to local solutions by updating an initial guess  $x^0$  using a search direction computed by solving the linear system in Equation (2.2), referred to as the KKT system.

$$(2.2) \quad \begin{bmatrix} \nabla^2 \mathcal{L} + \Sigma & \nabla f^T \\ \nabla f & \end{bmatrix} \begin{pmatrix} d_x \\ d_\lambda \end{pmatrix} = - \begin{pmatrix} \nabla \mathcal{L} \\ f \end{pmatrix}$$

Here,  $\mathcal{L}$  is the Lagrangian function,  $\lambda$  is the vector of Lagrange multipliers of the equality constraints, and  $\Sigma$  is a diagonal matrix containing the ratio of bound multipliers,  $\nu$ , to variable values. The matrix in Equation (2.2), referred to as the KKT matrix, is symmetric and indefinite.

**2.2. Inertia.** Interior point methods usually require linear algebra subroutines that can not only solve KKT systems but that can also compute the inertia of the KKT matrix. *Inertia* is defined as the numbers of positive, negative, and zero eigenvalues of a symmetric matrix. Inertia is often revealed by symmetric matrix factorization methods using Sylvester's Law of Inertia [62], which states that two congruent matrices have the same inertia. That is, if  $A$  and  $B$  are symmetric and  $R$  is nonsingular, then

$$(2.3) \quad A = R^T B R \Rightarrow \text{Inertia}(A) = \text{Inertia}(B)$$

**2.3. Schur complement.** The Schur complement is the matrix obtained by pivoting on a nonsingular submatrix. For a symmetric matrix

$$M = \begin{bmatrix} A & B^T \\ B & C \end{bmatrix}$$

with  $C$  nonsingular, the Schur complement of  $M$  with respect to  $C$  is

$$S = A - B^T C^{-1} B$$

When solving the linear system  $Mx = r$ , or

$$\begin{bmatrix} A & B^T \\ B & C \end{bmatrix} \begin{pmatrix} x_A \\ x_C \end{pmatrix} = \begin{pmatrix} r_A \\ r_C \end{pmatrix},$$

the Schur complement can be used to decompose the factorization and backsolve phases into steps involving only  $S$  or  $C$ , as shown in Algorithms 2.1 and 2.2.

---

**Algorithm 2.1** : Matrix factorization using the Schur complement
 

---

- 1: **Inputs:** Matrix  $M = \begin{bmatrix} A & B^T \\ B & C \end{bmatrix}$
  - 2: **factorize**( $C$ )
  - 3:  $S \leftarrow A - B^T C^{-1} B$
  - 4: **factorize**( $S$ )
  - 5: **Return:** **factors**( $C$ ), **factors**( $S$ )
- 

---

**Algorithm 2.2** : Backsolve using factors of the Schur complement
 

---

- 1: **Inputs:** **factors**( $C$ ), **factors**( $S$ ), right-hand side  $r = (r_A, r_C)$
  - 2:  $r_S \leftarrow r_A - B^T C^{-1} r_C$
  - 3:  $x_A \leftarrow S^{-1} r_S$
  - 4:  $\bar{r}_C \leftarrow r_C - B r_A$
  - 5:  $x_C \leftarrow C^{-1} \bar{r}_C$
  - 6: **Return:**  $x = (x_A, x_C)$
- 

The advantage of solving a system via this decomposition is that only matrices  $C$  and  $S$  need to be factorized, rather than the full matrix  $M$ . This is beneficial if the fill-in in  $A$  due to  $B^T C^{-1} B$  is relatively limited, that is, if a majority of  $B$ 's columns are empty, or if  $C$ 's structure can be exploited by a specialized algorithm.

When solving linear systems via a Schur complement, inertia is determined by the Haynsworth inertia additivity formula [35]:

$$(2.4) \quad \text{Inertia} \left( \begin{bmatrix} A & B^T \\ B & C \end{bmatrix} \right) = \text{Inertia}(C) + \text{Inertia}(A - B^T C^{-1} B).$$

**2.4. Block triangular decomposition.** An  $n \times n$  matrix  $M$  is *reducible* into block triangular form if it may be permuted (by row and column permutations  $P$  and  $Q$ ) to have the form

$$(2.5) \quad PMQ = \begin{bmatrix} M_{11} & 0 \\ M_{12} & M_{22} \end{bmatrix},$$

where  $M_{11}$  is  $k \times k$  and  $M_{22}$  is  $(n - k) \times (n - k)$  for some  $k$  between one and  $n - 1$ . That is,  $M$  is reducible if there exists a permutation that reveals a  $k \times (n - k)$  zero submatrix. (This definition is due to Frobenius [25]. Some sources, e.g., [54, 18], use the equivalent *Strong Hall Property*.) Here, the submatrices  $M_{11}$  and  $M_{22}$  may themselves be reducible. The problem of decomposing a matrix into irreducible block triangular form has been studied by Duff and Reid [23, 21], Gustavson [34], Howell [38], and others. When solving a linear system of equations defined by a reducible matrix, only the matrices on the diagonal need to be factorized. For example, when solving the system  $MX = B$ , where  $M$  decomposes into  $b$  blocks, i.e.,

$$\begin{bmatrix} M_{11} & & & \\ \vdots & \ddots & & \\ M_{1b} & \cdots & M_{bb} & \end{bmatrix} \begin{pmatrix} X_1 \\ \vdots \\ X_b \end{pmatrix} = \begin{pmatrix} B_1 \\ \vdots \\ B_b \end{pmatrix},$$

the following equation may be used to sequentially compute the blocks of the solution:

$$(2.6) \quad X_i = M_{ii}^{-1} \left( B_i - \sum_{j=1}^{i-1} M_{ji} X_j \right) \text{ for } i \text{ in } \{1, \dots, b\}.$$

The primary advantage of this procedure is that fill-in (nonzero entries that are present in a matrix's factors but not the matrix itself) is limited to the submatrices along the diagonal,  $M_{ii}$ , as these are the only matrices that are factorized. By contrast, a typical  $LU$  factorization of the matrix  $M$  above may have fill-in anywhere in or under the diagonal blocks. Additionally, L2 (matrix-vector) and L3 (matrix-matrix) BLAS are used directly in the backsolve procedure, Equation (2.6). In typical multifrontal and supernodal algorithms for symmetric-indefinite linear systems, performance benefits are obtained by aggregating rows and columns into dense submatrices on which L2 and L3 BLAS can efficiently operate. Exploiting a block triangular form (irreducible or otherwise) gives us more control over the data structures used to handle the off-diagonal submatrices. That is, these data structures may be sparse, dense, or some combination thereof and can be chosen to optimize the relatively simple matrix subtraction and multiplication operations in Equation (2.6), rather than chosen for performance in a more complicated factorization algorithm.

**2.5. Graphs of sparse matrices.** The sparsity pattern of an  $m \times n$  matrix may be represented as an undirected bipartite graph. One set of nodes represents the rows and the other represents the columns. There exists an edge  $(i, j)$  if the matrix entry at row  $i$  and column  $j$  is structurally nonzero.

For a square,  $n \times n$ , matrix, a directed graph on a single set of nodes  $\{1, \dots, n\}$  may be defined. The graph has a directed edge  $(i, j)$  if a structurally nonzero matrix entry exists at row  $i$  and column  $j$ .

These graphs are well-studied in the sparse matrix literature (see, e.g., [18]). In this work, they are necessary only for the statement and proof of Theorem 3.4.

**2.6. Neural networks.** The methods we use and develop in this work are applicable to general block triangular submatrices, including those found in multiperiod and discretized dynamic optimization problems. Here, we demonstrate the benefits of our approach on block triangular submatrices that arise in neural network-constrained optimization problems. These optimization problems arise in design and control with neural network surrogates, neural network verification, and adversarial example problems [49]. We address KKT matrices derived from nonlinear optimization problems with neural network constraints. A neural network,  $y = \text{NN}(x)$ , is a function defined by repeated application of an affine transformation and a nonlinear activation function  $\sigma$  over  $L$  layers:

$$(2.7) \quad y_l = \sigma_l(W_l y_{l-1} + b_l) \quad l \in \{1, \dots, L\},$$

where  $y_0 = x$  and  $y = y_L$ . In this context, training weights  $W_l$  and  $b_l$  are considered constant. We consider optimization problems with neural networks included in the constraints using a full-space formulation [58, 11, 20] in which intermediate variables and constraints are introduced for every layer of the neural network. The neural network constraints in our optimization problem are:

$$(2.8) \quad \left. \begin{array}{l} y_l = \sigma_l(z_l) \\ z_l = W_l y_{l-1} + b_l \end{array} \right\} \text{ for all } l \in \{1, \dots, L\}$$

We note that these neural network equations have a triangular incidence matrix. However, it is convenient to represent them in block triangular form, shown in Figure 1, where blocks correspond to layers of the neural network.

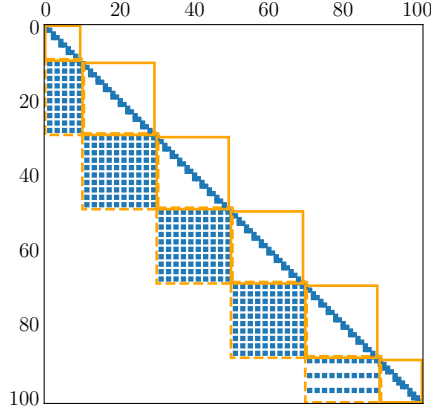


FIG. 1. Incidence matrix structure of neural network constraints. Rows are equations and columns are output or intermediate variables. Each box along the diagonal contains the variables (and constraints) for a particular layer of the network, i.e.,  $y_l$ ,  $z_l$ , and the associated constraints from Equation (2.8). The dashed boxes under the diagonal contain the nonzeros corresponding to the links between these variables and the variables of the next layer. That is they contain the  $W_l$  matrices from Equation (2.8).

### 3. Exploiting block triangularity within the Shur complement.

**3.1. Our approach.** We address KKT matrices derived from the following special case of Equation (2.1):

$$(3.1) \quad \begin{aligned} \min_{x,y} \quad & \varphi(x,y) \\ \text{subject to} \quad & f(x,y) = 0 \\ & g(x,y) = 0 \\ & L \leq (x,y) \leq U \end{aligned}$$

Here, we assume that  $\nabla_y g$  is nonsingular and block-lower triangular (with square, nonsingular blocks along the diagonal). Let the row and column dimensions of  $\nabla_y g$  be  $n_y$ . The KKT system of Equation (3.1) is:

$$(3.2) \quad \left[ \begin{array}{cc|cc} W_{xx} & \nabla_x f^T & W_{xy} & \nabla_x g^T \\ \nabla_x f & & \nabla_y f & \\ \hline W_{yx} & \nabla_y f^T & W_{yy} & \nabla_y g^T \\ \nabla_x g & & \nabla_y g & \end{array} \right] \begin{pmatrix} d_x \\ d_{\lambda_f} \\ d_y \\ d_{\lambda_g} \end{pmatrix} = - \begin{pmatrix} \nabla_x \mathcal{L} \\ f \\ \nabla_y \mathcal{L} \\ g \end{pmatrix}$$

Partitioning Equation (3.2) as shown above, we rewrite the system as Equation (3.3) for simplicity.

$$(3.3) \quad \begin{bmatrix} A & B^T \\ B & C \end{bmatrix} \begin{pmatrix} d_A \\ d_C \end{pmatrix} = \begin{pmatrix} r_A \\ r_C \end{pmatrix}$$

We will solve KKT systems of this form by performing a Schur complement reduction with respect to submatrix  $C$ , which we refer to as the *pivot matrix*. Because  $\nabla_y g$



this aggregation, diagonal blocks are themselves diagonal and off-diagonal blocks are either diagonal matrices containing derivatives of activation functions or the dense weight matrices that serve as inter-layer connections. Because the diagonal blocks are identity matrices, they do not need to be factorized and the block triangular back-solve procedure, Equation (2.6), will incur no fill-in. Furthermore, the off-diagonal matrices,  $M_{ji}$  in Equation (2.6), are either diagonal or fully dense. We store these dense matrices as contiguous arrays (rather than with a COO or CSC sparse matrix data structure) to take advantage of efficient L3 BLAS operations.

Finally, we observe that for the case of a neural network’s Jacobian, Equation (2.6) is very similar to the forward pass through the network:  $X_j$  is the solution for a previous layer’s intermediate variables,  $M_{ji}$  is the inter-layer weight matrix, and the backsolve with  $M_{ii}$  takes the place of an activation function.

**3.3. Fill-in.** The core benefit of our proposed algorithm is that we do not have to factorize the pivot matrix,  $C$ , directly. Instead, we factorize only the diagonal blocks of  $C$ ’s block triangular form,  $C_{ii}$ , and therefore only incur fill-in in these blocks. As we will show, this procedure incurs significantly less fill-in than we expect when factorizing the symmetric matrix  $C$  directly. Constructing the Schur complement matrix  $S$ , however, incurs fill-in in the columns of  $B$  that are nonzero.<sup>2</sup> Therefore, our method is particularly effective when the number of nonzero columns of  $B$ , i.e., the number of variables and constraints “linking”  $A$  and  $C$ , is small. We will now show that  $1 \times 1$  and  $2 \times 2$  pivots used by traditional symmetric indefinite linear solvers do not capture the structure of  $C$  and lead to fill-in outside of its diagonal blocks.

For simplicity, we rewrite  $C$  in its symmetric form as

$$C = \begin{bmatrix} D & E^T \\ E & \end{bmatrix},$$

then partition  $D$  and  $E$ :

$$D = \begin{bmatrix} d_{11} & D_{21}^T & D_{31}^T \\ D_{21} & D_{22} & D_{32}^T \\ D_{31} & D_{32} & D_{33} \end{bmatrix} \quad \text{and} \quad E = \begin{bmatrix} e_{11} & E_{12} & E_{13} \\ E_{21} & E_{22} & E_{23} \\ & & E_{33} \end{bmatrix}.$$

Here,  $d_{11}$  and  $e_{11}$  are scalars corresponding to a pivot and  $\begin{bmatrix} e_{11} & E_{12} \\ E_{21} & E_{22} \end{bmatrix}$  and  $E_{33}$  are two square diagonal blocks in a block triangular form of  $E$ . Submatrix  $E_{22}$  has the rows and columns that are in the same diagonal block as our pivot while  $E_{33}$  has row and column indices that are in a different diagonal block. With our proposed algorithm, fill-in is limited to these diagonal blocks. That is, our algorithm incurs no fill-in in  $E_{13}$ ,  $E_{23}$ , their transposes, or  $D$ . In the rest of this section, we will show that  $1 \times 1$  or  $2 \times 2$  pivots lead to fill-in in  $D$  and in the  $E_{23}$  and  $E_{23}^T$  blocks.

Applying permutation matrix  $P$  to put a potential  $2 \times 2$  pivot involving  $e_{11}$  in

---

<sup>2</sup>See the dense blocks in the Schur complement matrices in Figures 3 to 5. In our neural network application, these dense blocks correspond to the neural network’s inputs and the constraints containing any output of the network.



Any nonzero entries in the second term that are not in the first term are fill-in. These entries may exist in any of the nonzero blocks of the second term, which are limited to the  $D_{22}$ ,  $E_{22}$ ,  $D_{23}$ ,  $E_{23}$ , and  $D_{33}$  blocks of the original matrix (and their transposes).  $\square$

Theorems 3.1 and 3.2 apply to pivots induced by permuting  $E$  to block upper-triangular form. A similar result holds when  $E$  is initially in block-*lower* triangular form. We do not claim that either of these will result in a minimum-fill ordering or even that our results prove that a  $2 \times 2$  pivot is always strictly better than a  $1 \times 1$  pivot, as this will depend on sparsity patterns of the submatrices. However, these block-fill-in analyses give us reason to prefer a  $2 \times 2$  pivot involving  $e_{11}$  to a  $1 \times 1$  pivot. Our experience, which we justify with results in Subsection 5.2, is that traditional symmetric indefinite linear solvers prioritize  $1 \times 1$  pivots. We hypothesize that this is one reason for the large fill-in we will observe. We again highlight that neither  $1 \times 1$  nor  $2 \times 2$  pivots obtain the favorable result of our specialized method that fill-in is limited to diagonal blocks of  $E$ .

**3.4. Inertia and regularization.** Interior point methods require linear algebra subroutines that can not only solve KKT systems but that can also compute the inertia of the KKT matrix. As discussed in Subsection 2.3, Schur complement methods typically use the Haynsworth formula to check inertia given the inertia of the factorized pivot and Schur complement matrices. However, our block triangular factorization of  $C$  does not reveal its inertia. Fortunately, our assumption that  $\nabla_y g$  is nonsingular implies that the inertia of  $C$  is  $(n_y, n_y, 0)$  via Theorem 3.3 (a special case of Lemma 3.2 in [32]).

**THEOREM 3.3.** *Let  $C$  be as defined in Equation (3.3):*

$$C = \begin{bmatrix} W_{yy} & \nabla_y g^T \\ \nabla_y g & \end{bmatrix},$$

where  $\nabla_y g$  is  $n_y \times n_y$  and nonsingular. The inertia of  $C$  is  $(n_y, n_y, 0)$ .

*Proof of Theorem 3.3.* Let

$$R = \begin{bmatrix} I & -\frac{1}{2}W_{yy}\nabla_y g^{-1} \\ & \nabla_y g^{-1} \end{bmatrix}.$$

Then

$$RCR^T = \begin{bmatrix} & I \\ I & \end{bmatrix}.$$

The matrix  $\begin{bmatrix} & I \\ I & \end{bmatrix}$ , where  $I$  is  $n_y \times n_y$ , has inertia  $(n_y, n_y, 0)$ . Then, because  $R$  is nonsingular, by Sylvester's Law of Inertia,  $C$  has inertia  $(n_y, n_y, 0)$  as well.  $\square$

The inertia of  $C$  is therefore known *a priori*, so as long as an inertia-revealing method (i.e., an  $LBL^T$  factorization) is used for the factorization of the Schur complement matrix, we can recover the inertia of the original matrix as well.

Interior point methods use inertia to check conditions required for global convergence. In particular, the search direction computed must be a descent direction for the barrier objective function when projected into the null space of the equality constraint Jacobian [64]. This condition is met if the inertia of the KKT matrix is  $(n, m, 0)$ , where  $n$  is the number of variables and  $m$  is the number of equality constraints. If the KKT matrix is factorized and the inertia is incorrect, a multiple of the

identity matrix is added to the (1, 1) or (2, 2) block of the KKT matrix, depending on whether more positive or negative eigenvalues are needed.

While inertia correction is necessary for convergence of interior point methods, adding multiples of the identity matrix to  $C$  causes it to lose its property of reducibility. This is formalized in Theorem 3.4.

**THEOREM 3.4.** *Let  $S$  be the following symmetric, block- $2 \times 2$  matrix:*

$$S = \begin{bmatrix} I & B^T \\ B & I \end{bmatrix}.$$

*Let  $G_B$  be the bipartite graph of  $B$ . If  $G_B$  is connected, then  $S$  is irreducible.*

We use the following theorem (Varga [63], Theorem 1.17):

**THEOREM 3.5.** *Let  $M$  be an  $n \times n$  matrix and  $G$  its directed graph.  $M$  is irreducible if and only if  $G$  is strongly connected.*

*Proof of Theorem 3.4.* By Theorem 3.5, it is sufficient to show that the directed graph of  $S$ ,  $G_S$ , is strongly connected. Let  $n$  be the row and column dimension of  $B$ . The lower-left block,  $B$ , adds edges from  $\{1, \dots, n\}$  to  $\{n+1, \dots, 2n\}$  (corresponding to nonzero entries of  $B$ ) to  $G_S$  while the upper-right block,  $B^T$ , adds the reverse edges. We compress these pairs of edges to form an undirected graph, where connectivity in the undirected graph is equivalent to strong connectivity in the directed graph. This undirected graph is identical to  $B$ 's bipartite graph,  $G_B$ , with the following node mapping: Nodes  $\{1, \dots, n\}$  in  $G_S$  map to column nodes in  $G_B$  while  $\{n+1, \dots, 2n\}$  in  $G_S$  map to row nodes in  $G_B$ . Therefore connectivity of  $G_B$  implies strong connectivity of  $G_S$ , which (by Theorem 3.5) is equivalent to irreducibility of  $S$ .  $\square$

The regularized form of our pivot matrix, denoted  $\tilde{C}$ , is:

$$\tilde{C} = \begin{bmatrix} W_{yy} + \delta_y I & \nabla_y g^T \\ \nabla_y g & \delta_g I \end{bmatrix}.$$

Submatrix  $\nabla_y g$  is the Jacobian of neural network constraints and has a connected bipartite graph. Then by Theorem 3.4,  $\tilde{C}$  does not decompose via block triangularization. Therefore, we do not add regularization terms in the pivot matrix. We assume  $\nabla_y g$  is nonsingular, so regularization is not necessary to correct zero eigenvalues.

**4. Test problems.** We test our method on KKT matrices from three optimization problems involving neural network constraints: Adversarial generation for an MNIST image classifier (denoted “MNIST”), security-constrained optimal power flow with transient feasibility encoded by a neural network surrogate (denoted “SCOPF”), and load shed verification of power line switching decisions made by a neural network (denoted “LSV”). Structural properties of the neural networks and resulting optimization problems are shown in Tables 1 and 2.

**4.1. Adversarial image generation (MNIST).** The MNIST set of handwritten digits [44] is a set of images of handwritten digits commonly used in machine learning benchmarks. We have trained a set of neural networks to classify these images using PyTorch [53] and the Adam optimizer [42]. The networks each accept a  $28 \times 28$  grayscale image and output scores for each digit, 0-9, that may be interpreted as a probability of the image being that digit. The total numbers of neurons and trained parameters in the three networks we test for this problem are shown in Table 1. After training these neural networks, our goal is to find a minimal perturbation

TABLE 1  
*Properties of neural network models used in this work*

Model	N. inputs	N. outputs	N. neurons	N. layers	N. param.	Activation
MNIST	784	10	3k	7	1M	Tanh+SoftMax
			5k	7	5M	Tanh+SoftMax
			11k	7	18M	Tanh+SoftMax
SCOPF	117	37	1k	5	578k	Tanh
			5k	7	4M	Tanh
			12k	10	15M	Tanh
LSV	423	186	993	5	111k	Sigmoid
			2k	5	837k	Sigmoid
			6k	5	9M	Sigmoid

TABLE 2  
*Structure of optimization problems with different neural networks embedded*

Model	N. param.	N. var.	N. con.	Jac. NNZ	Hess. NNZ
MNIST	1M	7k	5k	1M	2k
	5M	12k	11k	5M	5k
	18M	22k	21k	18M	10k
SCOPF	578k	4k	4k	567k	9k
	4M	11k	11k	4M	12k
	15M	25k	25k	15M	19k
LSV	111k	8k	4k	125k	4k
	837k	10k	6k	854k	5k
	9M	19k	15k	9M	10k

to a reference image that results in a particular misclassification. This optimization problem is given by Equation (4.1), which is inspired by the minimal-adversarial-input formulations of Modas et al. [50] and Croce and Hein [16].

$$(4.1) \quad \begin{aligned} \min_x \quad & \|x - x_{\text{ref}}\|_1 \\ \text{subject to} \quad & y = \text{NN}(x) \\ & y_t \geq 0.6 \end{aligned}$$

Here,  $x \in \mathbb{R}^{784}$  contains grayscale values of the generated image and  $x_{\text{ref}}$  contains those of the reference image. Vector  $y \in \mathbb{R}^{10}$  contains the output score of each digit and  $t$  is the coordinate corresponding to the (misclassified) target label of the generated image. We note that  $t$  is a constant parameter chosen at the time we formulate the problem. We enforce that the new image is classified as the target with a probability of at least 60%. The sparsity structures of this problem’s KKT, pivot, and Schur complement matrices are shown in Figure 3.

**4.2. Security-constrained AC optimal power flow (SCOPF).** Security-constrained alternating current (AC) optimal power flow (SCOPF) is an optimization problem for dispatching generators in an electric power grid in which feasibility of the grid (with respect to voltage, line flow, and load satisfaction constraints) is enforced for a set of *contingencies*  $k \in K$  [3]. Each contingency represents the loss of a set

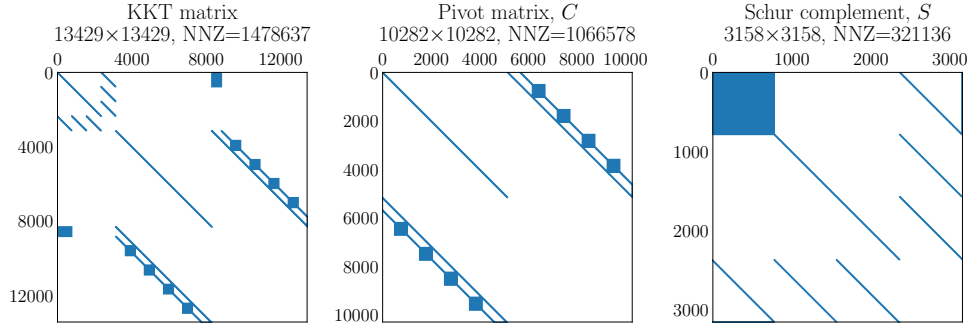


FIG. 3. Structure of KKT, pivot, and Schur complement matrices for the smallest instance of the MNIST test problem. The KKT matrix is in the order shown in Equation (3.2).

of generators and/or power lines. Instead of enforcing feasibility at the grid’s new steady state, we enforce feasibility of the first 30 seconds of the transient response. Specifically, we enforce that the frequency at each bus remains above  $\eta = 59.4$  Hz. Instead of inserting differential equations describing transient grid behavior into the optimization problem (as done by, e.g., Gan et al. [26]), we use a neural network that predicts the minimum frequency over this horizon. A simplified formulation is given in Equation (4.2):

$$(4.2) \quad \begin{aligned} & \min_{S^g, V} && c(\mathbb{R}(S^g)) \\ & \text{subject to} && \left. \begin{aligned} F_k(S^g, V, S^d) \leq 0 & \quad k \in \{0, \dots, K\} \\ y_k = \text{NN}_k(x) & \\ y_k \geq \eta & \end{aligned} \right\} \quad k \in \{1, \dots, K\} \end{aligned}$$

Here,  $S^g$  is a vector of complex AC power generations for each generator in the network,  $V$  is a vector of complex bus voltages,  $c$  is a quadratic cost function, and  $S^d$  is a constant vector of complex power demands. Constraint  $F_k \leq 0$  represents the set of constraints enforcing feasibility of the power network for contingency  $k$  (see [9]), where  $k = 0$  refers to the base-case network, and  $\text{NN}_k$  is the neural network function predicting minimum frequency following contingency  $k$ . This formulation is inspired by that of Garcia et al. [27]. We consider a simple instance of Equation (4.2) defined on a 37-bus synthetic test grid [7, 6] with a single contingency outaging generator 5 on bus 23. Here, the neural network has 117 inputs and 37 outputs. This surrogate is trained on data from 110 high-fidelity simulations using PowerWorld [55] with generations and loads uniformly sampled from within a  $\pm 20\%$  interval of each nominal value. These neural networks have between five and ten layers and between 500 and 1,500 neurons per layer (see Table 1). The sparsity structures of this problem’s KKT, pivot, and Schur complement matrices are shown in Figure 4.

**4.3. Line switching verification (LSV).** Our final test problem maximizes load shed due to line switching decisions made by a neural network that accepts loading conditions and wildfire risk (for every bus in a power network) as inputs. This is Problem 3 presented by Chevalier et al. [12]. The goal of the problem in [12] is to maximize load shed due to neural network switching decisions and an operator that acts to minimize a combination of load shed and wildfire risk. This bilevel

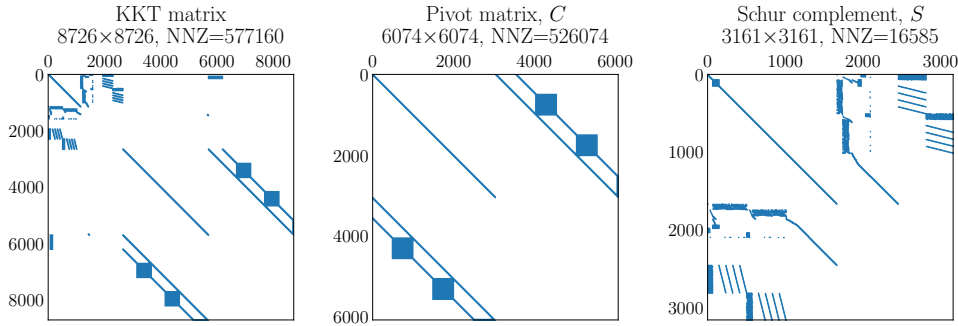


FIG. 4. Structure of KKT, pivot, and Schur complement matrices for the smallest instance of the SCOPF test problem.

problem is given by Equation (4.3).

$$(4.3) \quad \begin{aligned} & \max_{x, y, p_g} && C_1(x, y, p_g) \\ & \text{subject to} && y = \text{NN}(x) \\ & && p_g \in \underset{p_g \in \mathcal{F}(x, y)}{\text{argmin}} C_2(x, y, p_g) \end{aligned}$$

Here, both inner and outer problems are non-convex. The feasible set of the inner problem,  $\mathcal{F}(x, y)$ , is defined by the power flow equations with fixed loading,  $x$ , and line switching decisions,  $y$ . To approximate this problem with a single-level optimization problem, we follow [12] and relax the inner problem with a second-order cone relaxation [39], dualize the (now convex) inner problem, and combine the two levels of the optimization to yield a single-level nonconvex maximization problem. We refer the reader to [12] for further details, including a description of how these neural networks are trained.

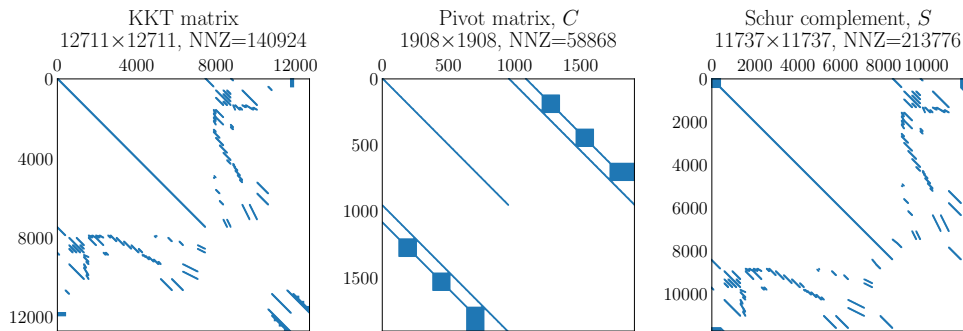


FIG. 5. Structure of KKT, pivot, and Schur complement matrices for the smallest instance of the LSV test problem.

## 5. Results.

**5.1. Computational setting.** Our method is implemented in Julia 1.11 [5]. Optimization models are implemented in JuMP [47], using PowerModels [14] and PowerModelsSecurityConstrained [13] for the SCOPF problem. Neural network models are trained using PyTorch and embedded into the JuMP models using MathOptAI [20]. KKT matrices are extracted from each optimization problem using MadNLP

[60, 59, 61] and we use block triangular and block-diagonal decompositions provided by MathProgIncidence [52]. We compare our method against the HSL MA57 [22] and MA86 [36] linear solvers. While MA86 can exploit parallel processing of the assembly tree and our algorithm can exploit L3 BLAS (matrix-matrix operations) parallelism, we run all experiments with a single processor in order to make a constant-hardware comparison. This is done by setting the number of OMP threads (used by MA86) to one and with the following Julia options:

```
LinearAlgebra.BLAS.set_num_threads(1)
LinearAlgebra.BLAS.lbt_set_num_threads(1)
```

These results were produced using the Selene supercomputer at Los Alamos National Laboratory on a compute node with two Intel 8468V 3.8 GHz processors and 2TB of RAM. Code and instructions to reproduce these results can be found at <https://github.com/Robbybp/moai-examples>.

**5.2. Numerical results.** To evaluate our method for each combination of optimization problem and neural network, we extract KKT matrices (and corresponding right-hand-sides) from the first ten iterations of the MadNLP interior point method<sup>3</sup> and compare the performance of our method with that of MA57 and MA86 on these linear systems. The KKT matrices at each iteration have the same structure, so we only perform a single symbolic factorization (referred to as “initialization”). Then we factorize the KKT matrix and backsolve with each of our ten KKT systems. Backsolves are repeated in iterative refinement until the max-norm of the residual is below  $10^{-5}$ . Table 3 reports the total time required, broken down into initialization, factorization, and backsolve steps for the ten linear systems as well as the average residual max-norm and average number of refinement iterations required. These backsolve runtimes include all refinement iterations. The speedup factor is a ratio of our solver’s runtime in the factorization plus backsolve phases to that of MA57 or MA86. We omit initialization time from this calculation as this step is amortized over many iterations of an interior point method. We note that our method computes the same inertia as MA57 or MA86 in every case.

Our method achieves lower factorization times at the cost of more expensive initializations and backsolves. Our faster factorizations make up for slower backsolves and achieve overall speedups between  $2.9\times$  and  $15\times$  for the largest neural networks considered even though more iterations of iterative refinement are sometimes required.

We hypothesize that our method outperforms MA57 and MA86 due to its limited fill-in when factorizing the block triangularizable pivot matrix. As discussed in Subsection 3.3, we expect MA57 and MA86 to incur significant fill-in when factorizing the original KKT matrix or the pivot matrix. Table 4 shows that this is the case. This table shows the size of the matrix factors and number of floating point operations required by these solvers on the original, pivot, and Schur complement matrices. For the original KKT and pivot matrices, MA57 and MA86 require factors 3-4 $\times$  larger than the original matrix. We attribute this fill-in partially to the relatively small number of  $2 \times 2$  pivots selected by these algorithms. The number of  $2 \times 2$  pivots is equal to about 25% of the matrix dimension, corresponding to about 50% of rows and columns in the factor matrices. Our analysis in Subsection 3.3 indicates that fill-in would be reduced if all of the pivots (at least in the pivot matrix) were  $2 \times 2$ .

While our method already outperforms MA57 and MA86 running on identical

---

<sup>3</sup>To make sure we compare different linear solvers on the same KKT systems, we always compute MadNLP’s search direction with our linear solver.

TABLE 3

Runtime results for ten KKT matrix factorizations for each model-solver combination. For each problem, we compare our method to a state-of-the-art alternative.

Model	Solver	NN param.	Total runtime (s)			Average		
			Init.	Fact.	Solve	Resid.	Refin. iter.	Speedup ( $\times$ )
MNIST	MA57	1M	0.04	2	0.1	2.7E-06	0	–
		5M	0.1	22	0.5	3.3E-07	0	–
		18M	1	125	2	1.3E-06	0	–
MNIST	Ours	1M	0.5	6	0.4	2.4E-08	1	0.25
		5M	3	12	1	8.2E-07	2	1.7
		18M	10	31	13	3.1E-06	7	2.9
SCOPF	MA86	578k	0.03	3	0.1	7.3E-07	1	–
		4M	0.2	32	1	2.9E-10	1	–
		15M	0.8	171	4	3.5E-10	1	–
SCOPF	Ours	578k	0.2	1	0.1	1.9E-06	1	2.6
		4M	2	3	0.7	1.4E-06	1	10
		15M	7	9	3	2.5E-08	1	15
LSV	MA86	111k	0.01	0.3	0.03	1.1E-08	0	–
		837k	0.04	5	0.1	6.8E-07	0	–
		9M	0.5	149	1	1.3E-06	0	–
LSV	Ours	111k	0.06	0.6	0.04	1.4E-06	0	0.51
		837k	0.4	3	0.3	2.1E-06	2	1.6
		9M	6	14	3	2.9E-06	3	8.8

TABLE 4

Factor sizes and floating point operations required to factorize KKT, pivot, and Schur complement matrices

Model	Solver	NN param.	Matrix	Matrix dim.	NNZ	Factor NNZ	FLOPs	N. 2 $\times$ 2 pivots
MNIST	MA57	18M	KKT	44k	18M	65M	177B	10k
			Pivot	41k	16M	50M	138B	10k
			Schur	3k	321k	323k	168M	0
SCOPF	MA86	15M	KKT	51k	16M	72M	127B	17k
			Pivot	48k	15M	71M	124B	17k
			Schur	3k	16k	104k	5M	1k
LSV	MA86	9M	KKT	36k	9M	44M	105B	13k
			Pivot	24k	8M	39M	84B	7k
			Schur	11k	213k	588k	136M	5k

hardware, there is significant opportunity to further improve our implementation. Table 5 shows a breakdown of runtime of the factorization and backsolve phases of our implementation. We first note that our factorization phase is dominated either by the cost to factorize the pivot matrix,  $C$ , or by the cost to build the Schur complement, i.e., performing the matrix subtraction, backsolve, and multiplication necessary to compute  $S = A - B^T C^{-1} B$ . These are the steps in lines 2 and 3 of Algorithm 2.1. When building the Schur complement, backsolves involving  $C$  (as described by Equation (2.6)) are the dominant computation cost. While the blocks of the solution matrix (or vector),  $X_i$ , need to be computed sequentially, the subtraction and multiplication operations used to construct these blocks (i.e.,  $B_i - \sum_{j=1}^{i-1} C_{ji} X_j$ ) can exploit single instruction, multiple data (SIMD) parallelism on multiple CPU cores or a GPU. De-

TABLE 5  
*Breakdown of solve times with our Schur complement solver*

Model	NN param.	Factorize (s)	Percent of factorize time (%)			Backsolve (s)
			Build Schur	Schur	Pivot	
MNIST	1M	6	88	1	6	0.4
	5M	13	76	1	17	2
	18M	32	70	0	26	13
SCOPF	578k	0.4	46	2	44	0.1
	4M	3	26	0	67	0.8
	15M	10	25	0	68	3
LSV	111k	0.6	72	14	3	0.05
	837k	2	84	3	9	0.3
	9M	15	65	0	29	3

pending on the structure of  $C_{ii}$  (i.e., if it is block-diagonal), the backsolve may be parallelized as well. Factorizing the individual diagonal blocks of the pivot matrix (i.e.,  $C_{ii}$ ) can also be parallelized.

**6. Conclusion.** We have shown that exploiting block triangular submatrices can yield up to  $15\times$  performance improvements when solving KKT systems compared to off-the-shelf multifrontal and supernodal methods. We have provided a theoretical justification for this speed up based on limited fill-in achieved with our method and have justified that the lack of inertia information from an unsymmetric block triangular solver is not prohibitive to using this method in nonlinear optimization methods. In fact, we have shown that our decomposition method will fail if inertia correction is attempted in the block triangular matrix that we exploit.

These results motivate several directions for future work. First, the methods we have developed can be applied to many other optimization problems with block triangular structures. For example, many sequential (dynamic or multi-period) optimization problems have this block triangular structure. Additionally, many problems that are not explicitly sequential may have large block triangular submatrices that can be exploited by our methods. We have shown in previous work that large triangular submatrices can be automatically identified [51]; future work should use Schur complement decompositions to exploit these submatrices in KKT systems. Additionally, the methods developed in [51] may be relaxed to automatically identify large *block*-triangular submatrices. Finally, a key advantage of our proposed method is that several of the computational bottlenecks (backsolving with the pivot matrix and constructing the Schur complement) can be parallelized on SIMD hardware. This decomposition should be implemented on GPUs with effort made to reduce CPU-GPU data transfer.

This work demonstrates that structure-exploiting decomposition algorithms can accelerate linear system solves even in the absence of advanced hardware. We intend this work to motivate research into additional structures that can be exploited in KKT systems. We believe that there is a significant opportunity improve performance of optimization algorithms through tighter integration between optimization problems and linear solvers. Here, we propose one method for improving performance in this way, although there is much that can be done to further develop this method and others.

**Acknowledgments.** This work was funded by the Los Alamos National Laboratory LDRD program under the Artemis project, the Center for Nonlinear Studies, and an ISTI Rapid Response award.

We thank Alexis Montoison for helpful conversations about our method, the HSL libraries, and an earlier draft of this manuscript.

**Appendix A. Size of submatrices.** Table 6 contains the dimensions and number of (structural) nonzero entries for KKT matrices and each submatrix considered in Equation (3.3).

**Appendix B. Comparison of linear solvers.** To justify our use of MA57 and MA86, we evaluate the time required to solve MadNLP’s KKT system at the initial guess with the solvers MA57 [22], MA86 [36], and MA97 [37] from the HSL library. The results are shown in Table 7. Each solver uses default options other than the pivot order, which we set to an approximate minimum degree (AMD) [1] variant with efficient handling of dense rows [2]. The results indicate that MA57 is the most performant solver for the MNIST test problem, while MA86 is most performant for the SCOPF and LSV problems. While MA86 and MA97 can exploit multicore parallelism, we run all solvers (including ours) with a single thread to make a constant-hardware comparison.

#### REFERENCES

- [1] P. R. AMESTOY, T. A. DAVIS, AND I. S. DUFF, *An approximate minimum degree ordering algorithm*, SIAM Journal on Matrix Analysis and Applications, 17 (1996), pp. 886–905, <https://doi.org/10.1137/S0895479894278952>.
- [2] P. R. AMESTOY, H. S. DOLLAR, J. K. REID, AND J. A. SCOTT, *An approximate minimum degree algorithm for matrices with dense rows*, Tech. Report RAL-TR-2004-015, Rutherford Appleton Laboratory, 2004.
- [3] I. ARAVENA, D. K. MOLZAHN, S. ZHANG, C. G. PETRA, F. E. CURTIS, S. TU, A. WÄCHTER, E. WEI, E. WONG, A. GHOLAMI, K. SUN, X. A. SUN, S. T. ELBERT, J. T. HOLZER, AND A. VEERAMANY, *Recent developments in security-constrained AC optimal power flow: Overview of challenge 1 in the ARPA-E grid optimization competition*, Operations Research, 71 (2023), pp. 1997–2014, <https://doi.org/10.1287/opre.2022.0315>.
- [4] M. BENZI, G. H. GOLUB, AND J. LIESEN, *Numerical solution of saddle point problems*, Acta Numerica, 14 (2005), p. 1–137, <https://doi.org/10.1017/S0962492904000212>.
- [5] J. BEZANSON, A. EDELMAN, S. KARPINSKI, AND V. B. SHAH, *Julia: A fresh approach to numerical computing*, SIAM Review, 59 (2017), pp. 65–98, <https://doi.org/10.1137/141000671>.
- [6] A. BIRCHFIELD, *Hawaii synthetic grid – 37 buses*, 2023, <https://electricgrids.engr.tamu.edu/hawaii40/>. Accessed 2024-12-10.
- [7] A. B. BIRCHFIELD, T. XU, K. M. GEGNER, K. S. SHETYE, AND T. J. OVERBYE, *Grid structural characteristics as validation criteria for synthetic networks*, IEEE Transactions on Power Systems, 32 (2017), pp. 3258–3265, <https://doi.org/10.1109/TPWRS.2016.2616385>.
- [8] J. R. BUNCH AND L. KAUFMAN, *Some stable methods for calculating inertia and solving symmetric linear systems*, Mathematics of Computation, (1977), pp. 163–179.
- [9] M. B. CAIN, R. P. O’NEILL, AND A. CASTILLO, *History of optimal power flow and formulations*, tech. report, Federal Energy Regulatory Commission, 2012.
- [10] L. CASACIO, C. LYRA, A. R. L. OLIVEIRA, AND C. O. CASTRO, *Improving the preconditioning of linear systems from interior point methods*, Computers & Operations Research, 85 (2017), pp. 129–138, <https://doi.org/https://doi.org/10.1016/j.cor.2017.04.005>, <https://www.sciencedirect.com/science/article/pii/S0305054817300965>.
- [11] F. CECCON, J. JALVING, J. HADDAD, A. THEBELT, C. TSAY, C. D. LAIRD, AND R. MISENER, *OMLT: Optimization & machine learning toolkit*, Journal of Machine Learning Research, 23 (2022), pp. 1–8, <http://jmlr.org/papers/v23/22-0277.html>.
- [12] S. CHEVALIER, D. STARKENBURG, R. PARKER, AND N. RHODES, *Maximal load shedding verification for neural network models of AC line switching*, 2025, <https://arxiv.org/abs/2510.23806>, <https://arxiv.org/abs/2510.23806>.

TABLE 6  
*Size of submatrices for each model and neural network*

Model	NN param.	Matrix	N. row	N. col	NNZ
MNIST	1M	KKT	13k	13k	1M
		$A$	3k	3k	5k
		$B$	10k	3k	401k
		Pivot matrix ( $C$ )	10k	10k	1M
		Schur complement ( $S$ )	3k	3k	321k
MNIST	5M	KKT	23k	23k	5M
		$A$	3k	3k	5k
		$B$	20k	3k	802k
		Pivot matrix ( $C$ )	20k	20k	4M
		Schur complement ( $S$ )	3k	3k	321k
MNIST	18M	KKT	44k	44k	18M
		$A$	3k	3k	5k
		$B$	41k	3k	1M
		Pivot matrix ( $C$ )	41k	41k	16M
		Schur complement ( $S$ )	3k	3k	321k
SCOPF	578k	KKT	9k	9k	578k
		$A$	3k	3k	10k
		$B$	6k	3k	39k
		Pivot matrix ( $C$ )	6k	6k	526k
		Schur complement ( $S$ )	3k	3k	16k
SCOPF	4M	KKT	23k	23k	4M
		$A$	3k	3k	10k
		$B$	20k	3k	78k
		Pivot matrix ( $C$ )	20k	20k	4M
		Schur complement ( $S$ )	3k	3k	16k
SCOPF	15M	KKT	51k	51k	16M
		$A$	3k	3k	10k
		$B$	48k	3k	117k
		Pivot matrix ( $C$ )	48k	48k	15M
		Schur complement ( $S$ )	3k	3k	16k
LSV	111k	KKT	13k	13k	142k
		$A$	11k	11k	28k
		$B$	1k	11k	54k
		Pivot matrix ( $C$ )	1k	1k	58k
		Schur complement ( $S$ )	11k	11k	213k
LSV	837k	KKT	18k	18k	876k
		$A$	11k	11k	28k
		$B$	6k	11k	216k
		Pivot matrix ( $C$ )	6k	6k	627k
		Schur complement ( $S$ )	11k	11k	213k
LSV	9M	KKT	36k	36k	9M
		$A$	11k	11k	28k
		$B$	24k	11k	866k
		Pivot matrix ( $C$ )	24k	24k	8M
		Schur complement ( $S$ )	11k	11k	213k

TABLE 7  
*Runtime of three linear solvers on the KKT matrix at the initial guess*

Model	Solver	NN param.	Initialize	Factorize	Backsolve	Residual
MNIST	MA57	1M	0.04	0.2	0.01	5.6E-10
		5M	0.2	2	0.05	9.5E-11
		18M	0.5	13	0.2	1.8E-11
	MA86	1M	0.06	0.7	0.02	6.7E-16
		5M	0.2	5	0.09	1.1E-15
		18M	1	30	0.3	6.1E-15
	MA97	1M	0.08	2	0.02	1.8E-15
		5M	0.4	15	0.08	9.1E-16
		18M*	–	–	–	–
SCOPF	MA57	578k	0.02	0.3	< 0.01	7.7E-09
		4M	0.1	5	0.05	5.9E-09
		15M	0.5	28	0.2	5.0E-09
	MA86	578k	0.02	0.3	0.01	5.3E-09
		4M	0.2	3	0.06	2.1E-09
		15M	0.8	17	0.3	1.8E-09
	MA97	578k	0.03	1	0.01	7.4E-09
		4M	0.3	11	0.06	2.9E-09
		15M*	–	–	–	–
LSV	MA57	111k	0.01	0.03	< 0.01	8.7E-11
		837k	0.2	0.7	0.01	2.8E-12
		9M <sup>†</sup>	–	–	–	–
	MA86	111k	0.01	0.03	< 0.01	4.4E-09
		837k	0.04	0.5	0.01	2.6E-12
		9M	0.5	15	0.2	2.0E-12
	MA97	111k	0.01	0.03	< 0.01	6.1E-11
		837k	0.05	1	0.01	4.5E-12
		18M*	–	–	–	–

\*Segmentation fault

<sup>†</sup>Int32 overflow

- [13] C. COFFRIN, *PowerModelsSecurityConstrained.jl*, 2022, <https://github.com/lanl-ansi/PowerModelsSecurityConstrained.jl>. Accessed 2024-12-10.
- [14] C. COFFRIN, R. BENT, K. SUNDAR, Y. NG, AND M. LUBIN, *PowerModels.jl: An open-source framework for exploring power flow formulations*, in 2018 Power Systems Computation Conference (PSCC), June 2018, pp. 1–8, <https://doi.org/10.23919/PSCC.2018.8442948>.
- [15] T. F. COLEMAN, *Large Sparse Numerical Optimization*, Lecture Notes in Computer Science, Springer, 1984.
- [16] F. CROCE AND M. HEIN, *Minimally distorted adversarial examples with a fast adaptive boundary attack*, ICML'20, JMLR.org, 2020.
- [17] F. E. CURTIS, O. SCHENK, AND A. WÄCHTER, *An interior-point algorithm for large-scale non-linear optimization with inexact step computations*, SIAM Journal on Scientific Computing, 32 (2010), pp. 3447–3475, <https://doi.org/10.1137/090747634>.
- [18] T. A. DAVIS, *Direct Methods for Sparse Linear Systems*, Society of Industrial and Applied Mathematics, 2006.
- [19] T. A. DAVIS AND I. S. DUFF, *An unsymmetric-pattern multifrontal method for sparse LU factorization*, SIAM Journal on Matrix Analysis and Applications, 18 (1997), pp. 140–158, <https://doi.org/10.1137/S0895479894246905>.
- [20] O. DOWSON, R. B. PARKER, AND R. BENT, *MathOptAI.jl: Embed trained machine learning*

- predictors into JuMP models*, 2025, <https://arxiv.org/abs/2507.03159>, <https://arxiv.org/abs/2507.03159>.
- [21] I. S. DUFF, *On permutations to block triangular form*, IMA Journal of Applied Mathematics, 19 (1977), pp. 339–342, <https://doi.org/10.1093/imamat/19.3.339>.
- [22] I. S. DUFF, *MA57—a code for the solution of sparse symmetric definite and indefinite systems*, 30 (2004), <https://doi.org/10.1145/992200.992202>.
- [23] I. S. DUFF AND J. K. REID, *An implementation of Tarjan’s algorithm for the block triangularization of a matrix*, ACM Trans. Math. Softw., 4 (1978), p. 137–147, <https://doi.org/10.1145/355780.355785>.
- [24] I. S. DUFF AND J. K. REID, *The multifrontal solution of indefinite sparse symmetric linear*, ACM Trans. Math. Softw., 9 (1983), p. 302–325, <https://doi.org/10.1145/356044.356047>.
- [25] F. G. FROBENIUS, *Über matrizen aus nicht negativen elementen*, Sitzungsberichte der Königlich Preussischen Akademie der Wissenschaften zu Berlin, 26 (1912), pp. 456–477.
- [26] D. GAN, R. THOMAS, AND R. ZIMMERMAN, *Stability-constrained optimal power flow*, IEEE Transactions on Power Systems, 15 (2000), pp. 535–540, <https://doi.org/10.1109/59.867137>.
- [27] M. GARCIA, N. LOGIUDICE, R. PARKER, AND R. BENT, *Transient stability-constrained OPF: Neural network surrogate models and pricing stability*, 2025, <https://arxiv.org/abs/2502.01844>, <https://arxiv.org/abs/2502.01844>.
- [28] G. GENG AND Q. JIANG, *A two-level parallel decomposition approach for transient stability constrained optimal power flow*, IEEE Transactions on Power Systems, 27 (2012), pp. 2063–2073, <https://doi.org/10.1109/TPWRS.2012.2190111>.
- [29] G. GENG, Q. JIANG, AND Y. SUN, *Parallel transient stability-constrained optimal power flow using gpu as coprocessor*, IEEE Transactions on Smart Grid, 8 (2017), pp. 1436–1445, <https://doi.org/10.1109/TSG.2016.2639551>.
- [30] G. H. GOLUB AND C. GREIF, *On solving block-structured indefinite linear systems*, SIAM Journal on Scientific Computing, 24 (2003), pp. 2076–2092, <https://doi.org/10.1137/S1064827500375096>.
- [31] J. GONDZIO AND R. SARKISSIAN, *Parallel interior-point solver for structured linear programs*, Mathematical Programming, 96 (2003), pp. 561–584, <https://doi.org/10.1007/s10107-003-0379-5>, <https://doi.org/10.1007/s10107-003-0379-5>.
- [32] N. I. M. GOULD, *On practical conditions for the existence and uniqueness of solutions to the general equality quadratic programming problem*, Mathematical Programming, 32 (1985), pp. 90–99, <https://doi.org/10.1007/BF01585660>, <https://doi.org/10.1007/BF01585660>.
- [33] M. D. GRIGORIADIS AND L. G. KHACHIYAN, *An interior point method for bordered block-diagonal linear programs*, SIAM Journal on Optimization, 6 (1996), pp. 913–932, <https://doi.org/10.1137/S1052623494263609>.
- [34] F. GUSTAVSON, *Finding the block lower triangular form of a sparse matrix*, in Sparse Matrix Computations, J. R. Bunch and D. J. Rose, eds., Academic Press, 1976, pp. 275–289, <https://doi.org/https://doi.org/10.1016/B978-0-12-141050-6.50021-0>.
- [35] E. V. HAYNSWORTH, *Determination of the inertia of a partitioned Hermitian matrix*, Linear Algebra and its Applications, 1 (1968), pp. 73–81, [https://doi.org/https://doi.org/10.1016/0024-3795\(68\)90050-5](https://doi.org/https://doi.org/10.1016/0024-3795(68)90050-5), <https://www.sciencedirect.com/science/article/pii/0024379568900505>.
- [36] J. D. HOGG AND J. A. SCOTT, *An indefinite sparse direct solver for large problems on multicore machines*, Tech. Report RAL-TR-2010-011, Rutherford Appleton Laboratory, 2010.
- [37] J. D. HOGG AND J. A. SCOTT, *HSL-MA97: a bit-compatible multifrontal code for sparse symmetric systems*, Tech. Report RAL-TR-2011-024, Rutherford Appleton Laboratory, 2011.
- [38] T. D. HOWELL, *Partitioning using PAQ++*, in Sparse Matrix Computations, J. R. Bunch and D. J. Rose, eds., Academic Press, 1976, pp. 23–37, <https://doi.org/https://doi.org/10.1016/B978-0-12-141050-6.50007-6>.
- [39] R. JABR, *Radial distribution load flow using conic programming*, IEEE Transactions on Power Systems, 21 (2006), pp. 1458–1459, <https://doi.org/10.1109/TPWRS.2006.879234>.
- [40] D. JIN, A. MONTOISON, AND S. SHIN, *Harnessing batched BLAS/LAPACK kernels on GPUs for parallel solutions of block tridiagonal systems*, 2025, <https://arxiv.org/abs/2509.03015>, <https://arxiv.org/abs/2509.03015>.
- [41] J. KANG, Y. CAO, D. P. WORD, AND C. LAIRD, *An interior-point method for efficient solution of block-structured NLP problems using an implicit Schur-complement decomposition*, Computers & Chemical Engineering, 71 (2014), pp. 563–573, <https://doi.org/https://doi.org/10.1016/j.compchemeng.2014.09.013>, <https://www.sciencedirect.com/science/article/pii/S0098135414002798>.
- [42] D. P. KINGMA AND J. BA, *Adam: A method for stochastic optimization*, 2017, <https://arxiv.org/abs/1712.07547>.

- org/abs/1412.6980, <https://arxiv.org/abs/1412.6980>.
- [43] C. D. LAIRD AND L. T. BIEGLER, *Large-scale nonlinear programming for multi-scenario optimization*, in Modeling, Simulation and Optimization of Complex Processes, H. G. Bock, E. Kostina, H. X. Phu, and R. Rannacher, eds., Berlin, Heidelberg, 2008, Springer Berlin Heidelberg, pp. 323–336.
- [44] Y. LECUN, C. CORTES, AND C. J. C. BURGES, *The MNIST database of handwritten digits*, (1998), <http://yann.lecun.com/exdb/mnist/>.
- [45] J. W. H. LIU, E. G. NG, AND B. W. PEYTON, *On finding supernodes for sparse matrix computations*, SIAM Journal on Matrix Analysis and Applications, 14 (1993), pp. 242–252, <https://doi.org/10.1137/0614019>.
- [46] F. J. LÓPEZ-FLORES, C. RAMÍREZ-MÁRQUEZ, AND J. PONCE-ORTEGA, *Process systems engineering tools for optimization of trained machine learning models: Comparative and perspective*, Industrial & Engineering Chemistry Research, 63 (2024), pp. 13966–13979, <https://doi.org/10.1021/acs.iecr.4c00632>, <https://doi.org/10.1021/acs.iecr.4c00632>.
- [47] M. LUBIN, O. DOWSON, J. D. GARCIA, J. HUCHETTE, B. LEGAT, AND J. P. VIELMA, *JuMP 1.0: Recent improvements to a modeling language for mathematical optimization*, Mathematical Programming Computation, 15 (2023), pp. 581–589, <https://doi.org/10.1007/s12532-023-00239-3>.
- [48] I. J. LUSTIG AND G. LI, *An implementation of a parallel primal-dual interior point method for block-structured linear programs*, Computational Optimization and Applications, 1 (1992), pp. 141–161, <https://doi.org/10.1007/BF00253804>, <https://doi.org/10.1007/BF00253804>.
- [49] F. J. LÓPEZ-FLORES, C. RAMÍREZ-MÁRQUEZ, AND J. M. PONCE-ORTEGA, *Process systems engineering tools for optimization of trained machine learning models: Comparative and perspective*, Industrial & Engineering Chemistry Research, 63 (2024), pp. 13966–13979, <https://doi.org/10.1021/acs.iecr.4c00632>.
- [50] A. MODAS, S.-M. MOOSAVI-DEZFOOLI, AND P. FROSSARD, *SparseFool: A few pixels make a big difference*, in 2019 IEEE/CVF Conference on Computer Vision and Pattern Recognition (CVPR), 2019, pp. 9079–9088, <https://doi.org/10.1109/CVPR.2019.00930>.
- [51] S. NAIK, L. BIEGLER, R. BENT, AND R. PARKER, *Variable aggregation for nonlinear optimization problems*, 2025, <https://arxiv.org/abs/2502.13869>, <https://arxiv.org/abs/2502.13869>.
- [52] R. B. PARKER, B. L. NICHOLSON, J. D. SHIROLA, AND L. T. BIEGLER, *Applications of the Dulmage–Mendelsohn decomposition for debugging nonlinear optimization problems*, Computers & Chemical Engineering, 178 (2023), p. 108383, <https://doi.org/https://doi.org/10.1016/j.compchemeng.2023.108383>, <https://www.sciencedirect.com/science/article/pii/S0098135423002533>.
- [53] A. PASZKE, S. GROSS, F. MASSA, A. LERER, J. BRADBURY, G. CHANAN, T. KILLEEN, Z. LIN, N. GIMELSHEIN, L. ANTIGA, ET AL., *Pytorch: An imperative style, high-performance deep learning library*, Advances in neural information processing systems, 32 (2019).
- [54] A. POTHEN AND C.-J. FAN, *Computing the block triangular form of a sparse matrix*, ACM Trans. Math. Softw., 16 (1990), p. 303–324, <https://doi.org/10.1145/98267.98287>.
- [55] POWERWORLD CORPORATION, *PowerWorld Simulator Manual*, Champaign, IL, USA. <https://www.powerworld.com/WebHelp/> Accessed December 10, 2024.
- [56] S. REGEV, N.-Y. CHIANG, E. DARVE, C. G. PETRA, M. A. SAUNDERS, K. ŚWIRYDOWICZ, AND S. PELEŠ, *HyKKT: a hybrid direct-iterative method for solving KKT linear systems*, Optimization Methods and Software, 38 (2023), pp. 332–355, <https://doi.org/10.1080/10556788.2022.2124990>.
- [57] L. SCHORK AND J. GONDZIO, *Implementation of an interior point method with basis preconditioning*, Mathematical Programming Computation, 12 (2020), pp. 603–635, <https://doi.org/10.1007/s12532-020-00181-8>, <https://doi.org/10.1007/s12532-020-00181-8>.
- [58] A. M. SCHWEIDTMANN AND A. MITSOS, *Deterministic global optimization with artificial neural networks embedded*, Journal of Optimization Theory and Applications, 180 (2019), pp. 925–948.
- [59] S. SHIN, M. ANITESCU, AND F. PACAUD, *Accelerating optimal power flow with GPUs: SIMD abstraction of nonlinear programs and condensed-space interior-point methods*, Electric Power Systems Research, 236 (2024), p. 110651, <https://doi.org/https://doi.org/10.1016/j.epr.2024.110651>.
- [60] S. SHIN, C. COFFRIN, K. SUNDAR, AND V. M. ZAVALA, *Graph-based modeling and decomposition of energy infrastructures*, IFAC-PapersOnLine, 54 (2021), pp. 693–698.
- [61] S. SHIN AND CONTRIBUTORS, *MadNLP.jl*, 2025, <https://github.com/MadNLP/MadNLP.jl>. Accessed 2025-09-04.
- [62] J. J. SYLVESTER, *A demonstration of the theorem that every homogeneous quadratic polynomial is reducible by real orthogonal substitutions to the form of a sum of positive and negative*

- squares*, Philosophical Magazine, 4 (1852), pp. 138–142.
- [63] R. S. VARGA, *Matrix Iterative Analysis*, Springer, second ed., 2000.
  - [64] A. WÄCHTER AND L. T. BIEGLER, *Line search filter methods for nonlinear programming: Motivation and global convergence*, SIAM Journal on Optimization, 16 (2005), pp. 1–31, <https://doi.org/10.1137/S1052623403426556>.
  - [65] S. J. WRIGHT, *Partitioned dynamic programming for optimal control*, SIAM Journal on Optimization, 1 (1991), pp. 620–642, <https://doi.org/10.1137/0801037>.
  - [66] F. ZANETTI AND J. GONDZIO, *A new stopping criterion for Krylov solvers applied in interior point methods*, SIAM Journal on Scientific Computing, 45 (2023), pp. A703–A728, <https://doi.org/10.1137/22M1490041>.
  - [67] K. ŚWIRYDOWICZ, E. DARVE, W. JONES, J. MAACK, S. REGEV, M. A. SAUNDERS, S. J. THOMAS, AND S. PELEŠ, *Linear solvers for power grid optimization problems: A review of GPU-accelerated linear solvers*, Parallel Computing, 111 (2022), p. 102870, <https://doi.org/https://doi.org/10.1016/j.parco.2021.102870>, <https://www.sciencedirect.com/science/article/pii/S0167819121001125>.